J|A|C|S COMMUNICATIONS

Published on Web 02/03/2009

A Stable Hyponitrite-Bridged Iron Porphyrin Complex

Nan Xu, Adam L. O. Campbell, Douglas R. Powell, Jana Khandogin,* and George B. Richter-Addo*

Department of Chemistry and Biochemistry, University of Oklahoma, 620 Parrington Oval, Norman, Oklahoma 73019

Received December 15, 2008; E-mail: jana.k.shen@ou.edu; grichteraddo@ou.edu

Heme-assisted coupling of nitric oxide (NO) to form Fe{N_2O_2}^{n} intermediates plays an important part in the reduction of NO to N_2O.[1,2] In transition-metal chemistry, such metal{N_2O_2}^{n} moieties can be generated from attack of NO on a metal-NO group,[3,4] from metal-induced coupling of NO,[5] or from transfer of an intact $(N_2O_2)^{n}$ from a diazeniumdiolate to a metal.[6] It is interesting to note that only a small number of metal{N_2O_2}-containing compounds have been structurally characterized, and the {N_2O_2} binding modes determined to date are sketched below as structures **A** (M = Pt, Ni),[5,6] **B** (M = M′ = Co),[7] **C** (M = Ru),[8] and **D** (M = Co).[9]

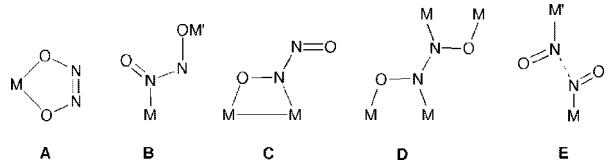

Enzymes such as the NO reductase (NOR) from *Paracoccus denitrificans*, cyt ba_3 and caa_3 from *Thermus thermophilus*, and cyt cbb_3 from *Paracoccus stutzeri* catalyze the conversion of NO to N_2O using bimetallic active sites.[1,2] For these biological systems, intermediates resembling structure **B** have been proposed, where the metal{N_2O_2} moiety is *N*-bound to heme Fe (M), and where M′ (nonheme Fe or Cu) may contact both O atoms.[1,10] Collman et al. have proposed, using results from the reaction of a diferrous synthetic model of NOR with NO, that a *trans*-bis-nitrosyl intermediate forms at the active site of NOR followed by NO coupling (structure **E**) to give N_2O and a bis-ferric product.[11] Resonance Raman spectroscopy has been employed to assign a HONNO-bridged Fe−Cu species (i.e., a protonated analogue of **E**) during NO reduction by *T. thermophilus* cyt ba_3.[12] To the best of our knowledge, however, no adduct of heme and an N_2O_2 moiety has been structurally characterized.

The title compound was obtained from the reaction of [(OEP)Fe]$_2$(μ-O) in anhydrous toluene with an in situ-generated ether solution of hyponitrous acid (Supporting Information) (eq 1). Workup gave the product [(OEP)Fe]$_2$(μ-N_2O_2) (**1**) as dark purple microcrystals in 52% isolated yield.

$$[(\mathrm{OEP})\mathrm{Fe}]_2(\mu\text{-O}) + \mathrm{H_2N_2O_2} \rightarrow [(\mathrm{OEP})\mathrm{Fe}]_2(\mu\text{-}\mathrm{N_2O_2}) + \mathrm{H_2O} \quad (1)$$

The IR spectrum of **1** reveals a band at 982 cm^{-1} assigned to ν_{as} of the N–O group (ν_{as}(^{15}NO) 973 cm^{-1}). This band is lower than that reported for $H_2N_2O_2$ at 1014/1003 cm^{-1} (ν_{as}(^{15}NO) 991/980 cm^{-1}).[13] The ν_s(NO) and ν(NN) bands were not observed in the IR spectrum, presumably due to the symmetry of **1**. The EPR spectrum of **1** as a CH_2Cl_2/toluene glass (77 K) shows g = 5.74 and 2.03; similar data were obtained for two high-spin (H.S.) ferric hydroxo porphyrins.[14]

The X-ray crystal structure of **1** reveals that the N_2O_2 ligand is bound to each Fe via the η^1-O binding mode and that the ONNO moiety is trans (Figure 1). The N−N bond length of 1.250(3) Å suggests double bond character (cf., 1.256(2) Å in crystalline $Na_2N_2O_2$).[15] The distance between the two Fe centers is 6.7 Å and is longer than the 4.4 Å distance between the Fe and Cu centers in *T. thermophilus* cyt ba_3 that exhibits NOR activity.[16] The magnitude of the Fe−N(por) bond lengths in **1** and the apical displacement of Fe from the 4N-atom porphyrin mean plane (ΔFe = 0.40 Å) are indicative of H.S. ferric centers. It follows that the N_2O_2 ligand in **1** must have significant hyponitrite (i.e., dianionic) character.

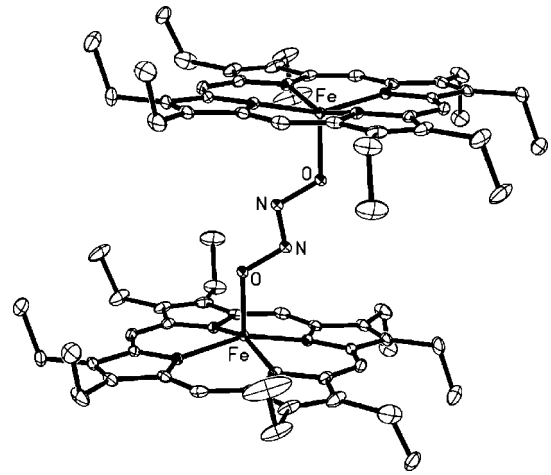

Figure 1. Molecular structure of [(OEP)Fe]$_2$(μ-ONNO) (**1**). Hydrogen atoms and the dichloromethane solvates have been omitted for clarity. Selected bond lengths (Å) and angles (deg): Fe−O = 1.889(2), O−N = 1.375(2), N−N = 1.250(3), Fe−N(por) = 2.049(2)−2.064(2), ∠FeON = 118.56(12), ∠NNO = 108.5(2).

To characterize the electronic structure and properties of **1**, we performed calculations using density functional theory (DFT) on the model compound [(porphine)Fe]$_2$(η^1,η^1,μ-N_2O_2) (**1**-calc) in the trans and cis configurations. The DFT calculations were based on the B3LYP exchange-correlation functional and a triple-ζ polarization basis set. In both trans and cis configurations, the H.S. species is calculated to be lower in energy relative to the intermediate- (I.S.) and low-spin (L.S.) variants by 8 and 19 kcal/mol, respectively (Table S2). The calculated geometry of the trans H.S. species most closely reproduces the crystal structural data (Table 1). Curiously, the different spin states of the trans isomer are calculated to be ∼2 kcal/mol higher in energy than the respective cis variants. This small difference lies within the typical error of 3−5 kcal/mol estimated for B3LYP calculations of transition-metal complexes. Thus, the DFT calculations are consistent with the EPR and structural data in establishing the identity of a stable H.S. trans species. The small energy gap between the trans and cis configurations suggests that isolation of the cis derivative of **1** might be attainable.

To probe the charge distribution in **1**, we used multipole-derived population analysis for the trans H.S. form of **1**-calc. The atomic

 10.1021/ja809781r CCC: $40.75

Table 1. Selected Crystal Data for **1**, and Calculated Geometry Data (in Å and deg) for [(Porphine)Fe]$_2$(η^1,η^1,μ-N_2O_2) (**1**-calc)

	Fe−O	O−N	N−N	∠NNO	ΔFe
1 (crystal; trans)	1.889	1.375	1.250	108.5	0.402
1-calc					
trans-H.S.	1.909	1.376	1.269	108.9	0.482
trans-I.S.	1.951	1.364	1.280	109.3	0.272
trans-L.S.	1.831	1.398	1.266	107.4	0.249
cis-H.S.	1.899	1.390	1.254	117.0	0.485
cis-I.S.	1.945	1.379	1.262	117.9	0.279
cis-L.S.	1.831	1.403	1.258	116.5	0.232

charges on the Fe, O, and N atoms are shown in Figure 2. To further understand the charge distribution in the FeONNOFe moiety, we used the Nalewajski−Mrozek scheme to calculate the bond orders. Accordingly, the bond orders for Fe−O, O−N, and N−N in **1**-calc trans-H.S. (Figure 2) are 0.79, 1.25, and 1.84, respectively, which supports the notion of an N═N double bond in the hyponitrite bridge.

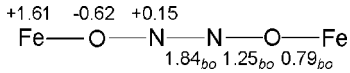

Figure 2. Calculated atomic charges and bond orders (bo) for the FeONNOFe moiety.

The Kohn−Sham orbitals of the trans H.S. species of **1**-calc are expected to be similar to those of square pyramidal metal complexes, for which the highest occupied orbital and the lowest unoccupied orbital are the result of antibonding interactions between d_{z^2} as well as $d_{(x^2-y^2)}$ orbitals of the metal and the symmetrized

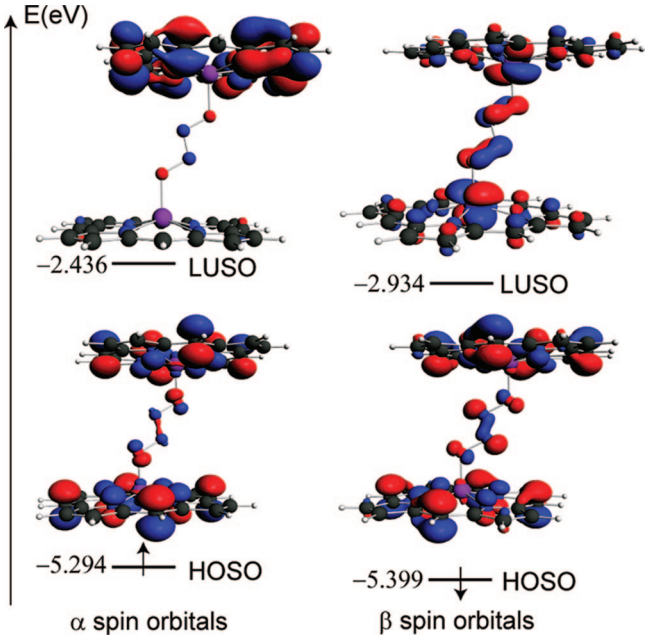

Figure 3. Frontier spin orbitals for high-spin **1**-calc. HOSO and LUSO denote the highest occupied and the lowest unoccupied spin orbitals, respectively.

combinations of the ligand σ orbitals. The frontier spin orbitals from the unrestricted open-shell calculation are shown in Figure 3. The highest occupied α spin orbital exhibits more porphine character while the lowest unoccupied spin β orbital displays more metal character. The N atoms of the hyponitrite bridge form a bonding interaction in both highest occupied spin orbitals.

Protonation of a toluene solution of **1** at 0 °C using HCl results in the formation of N_2O and (OEP)FeCl (eq 2).

$$[(OEP)Fe]_2(\mu\text{-ONNO}) + 2HCl \rightarrow N_2O + 2(OEP)FeCl + H_2O \quad (2)$$

An IR spectrum of the headspace reveals new bands at 2236/2213 and 1298/1266 cm^{-1} assigned to υ_{as} and υ_s of N_2O, respectively. The use of the ^{15}N-labeled **1** (labeled at hyponitrite) shifts the υ_{as} bands to 2167/2144 cm^{-1}; the corresponding υ_s bands were not observed due to its occurrence outside the detection window.

We hypothesized that the protonation reaction is initiated by H^+ attack on one of the O atoms of the hyponitrite bridge followed by O−N bond cleavage to give N_2O. This is supported by the pronounced negative charge on the hyponitrite O atom in trans-H.S. **1**-calc obtained from the DFT calculation. Further studies are underway to uncover the mechanism of the protonation reaction.

In summary, we have prepared and characterized the first isolable hyponitrite iron porphyrin complex and describe the first established hyponitrite *O*-bonding mode to a heme model.

Acknowledgment. We are grateful to the National Institutes of Health for funding (GM076640; GBR-A).

Supporting Information Available: Experimental procedure, computational details, additional references, and CIF file for **1**. This material is available free of charge via the Internet at http://pubs.acs.org.

References

(1) Moenne-Loccoz, P. *Nat. Prod. Rep.* **2007**, *24*, 610–620.
(2) Yeung, N.; Lu, Y. *Chem. Biodiversity* **2008**, *5*, 1437–1454.
(3) Franz, K. J.; Lippard, S. J. *J. Am. Chem. Soc.* **1999**, *121*, 10504–10512.
(4) Schneider, J. L.; Carrier, S. M.; Ruggiero, C. E.; Young, V. G.; Tolman, W. B. *J. Am. Chem. Soc.* **1998**, *120*, 11408–11418.
(5) Arulsamy, N.; Bohle, D. S.; Imonigie, J. A.; Moore, R. C. *Polyhedron* **2007**, *26*, 4737–4745.
(6) Arulsamy, N.; Bohle, D. S.; Imonigie, J. A.; Levine, S. *Angew. Chem., Int. Ed.* **2002**, *41*, 2371–2373.
(7) Villalba, M. E. C.; Navaza, A.; Guida, J. A.; Varetti, E. L.; Aymonino, P. J. *Inorg. Chim. Acta* **2006**, *359*, 707–712.
(8) Bottcher, H.-C.; Graf, M.; Mereiter, K.; Kirchner, K. *Organometallics* **2004**, *23*, 1269–1273.
(9) Bau, R.; Sabherwal, I. H.; Burg, A. B. *J. Am. Chem. Soc.* **1971**, *93*, 4926–4928.
(10) Blomberg, L. M.; Blomberg, M. R. A.; Siegbahn, P. E. M. *Biochim. Biophys. Acta* **2006**, *1757*, 31–46.
(11) Collman, J. P.; Dey, A.; Yang, Y.; Decreau, R. A.; Ohta, T.; Solomon, E. I. *J. Am. Chem. Soc.* **2008**, *130*, 16498–16499.
(12) Varotsis, C.; Ohta, T.; Kitagawa, T.; Soulimane, T.; Pinakoulaki, E. *Angew. Chem., Int. Ed.* **2007**, *46*, 2210–2214.
(13) McGraw, G. E.; Bernitt, D. L.; Hisatsune, I. C. *Spectrochim. Acta* **1967**, *23A*, 25–34.
(14) Cheng, R.-U.; Latos-Grazynski, L.; Balch, A. L. *Inorg. Chem.* **1982**, *21*, 2412–2418.
(15) Arulsamy, N.; Bohle, D. S.; Imonigie, J. A.; Sagan, E. S. *Inorg. Chem.* **1999**, *38*, 2716–2725.
(16) Soulimane, T.; Buse, G.; Bourenkov, G. P.; Bartunik, H. D.; Huber, R.; Than, M. E. *Embo J.* **2000**, *19*, 1766–1776.

JA809781R